

Ultrastructural Localization of GPR179 and the Impact of Mutant Forms on Retinal Function in CSNB1 Patients and a Mouse Model

Jan Klooster,¹ Maria M. van Genderen,² Minzhong Yu,³ Ralph J. Florijn,⁴ Frans C. C. Riemsdag,² Arthur A. B. Bergen,⁴⁻⁶ Ronald G. Gregg,⁷ Neal S. Peachey,^{3,8,9} and Maarten Kamermans^{1,10}

¹Retinal Signal Processing, Netherlands Institute for Neuroscience, Amsterdam, The Netherlands

²Bartiméus, Zeist, The Netherlands

³Department of Ophthalmic Research, Cole Eye Institute, Cleveland Clinic, Cleveland, Ohio

⁴Ophthalmogenetics, Netherlands Institute for Neuroscience, Amsterdam, The Netherlands

⁵Department of Ophthalmology, Academic Medical Center, Amsterdam, The Netherlands

⁶Department of Clinical Genetics, Academic Medical Center, Amsterdam, The Netherlands

⁷Departments of Biochemistry & Molecular Biology and Ophthalmology & Visual Sciences, University of Louisville, Louisville, Kentucky

⁸Research Service, Louis Stokes Cleveland VA Medical Center, Cleveland, Ohio

⁹Department of Ophthalmology, Cleveland Clinic Lerner College of Medicine of Case Western Reserve University, Cleveland, Ohio

¹⁰Department of Neurogenetics, Academic Medical Center, Amsterdam, The Netherlands

Correspondence: Maarten Kamermans, Netherlands Institute for Neuroscience, Retinal Signal Processing Group, Meibergdreef 47, 1105 BA Amsterdam, The Netherlands; m.kamermans@nin.knaw.nl

JK, MMvG, and MY contributed equally to the work presented here and should therefore be regarded as equivalent authors.

Submitted: April 25, 2013

Accepted: September 12, 2013

Citation: Klooster J, van Genderen MM, Yu M, et al. Ultrastructural localization of GPR179 and the impact of mutant forms on retinal function in CSNB1 patients and a mouse model. *Invest Ophthalmol Vis Sci*. 2013;54:6973-6981. DOI: 10.1167/iovs.13-12293

PURPOSE. Complete congenital stationary night blindness (CSNB1) is characterized by loss of night vision due to a defect in the retinal ON-bipolar cells (BCs). Mutations in *GPR179*, encoding the G-protein-coupled receptor 179, have been found in CSNB1 patients. In the mouse, *GPR179* is localized to the tips of ON-BC dendrites. In this study we determined the ultrastructural localization of *GPR179* in human retina and determined the functional consequences of mutations in *GPR179* in patients and mice.

METHODS. The localization of *GRP179* was analyzed in postmortem human retinas with immunohistochemistry. The functional consequences of the loss of *GPR179* were analyzed with standard and 15-Hz flicker ERG protocols.

RESULTS. In the human retina, *GPR179* is localized on the tips of ON-BC dendrites, which invaginate photoreceptors and terminate juxtaposed to the synaptic ribbon. The 15-Hz flicker ERG abnormalities found in patients with mutations in *GPR179* more closely resemble those from patients with mutations in either *TRPM1* or *NYX* than in *GRM6*. 15-Hz flicker ERG abnormalities of *Gpr179^{nob5}* and *Grm6^{nob3}* mice were comparable.

CONCLUSIONS. *GRP179* is expressed on dendrites of ON-BCs, indicating that *GRP179* is involved in the ON-BCs' signaling cascade. The similarities of 15-Hz flicker ERGs noted in *GPR179* patients and *NYX* or *TRPM1* patients suggest that the loss of *GPR179* leads to the loss or closure of *TRPM1* channels. The difference between the 15-Hz flicker ERGs of mice and humans indicates the presence of important species differences in the retinal activity that this signal represents.

Keywords: *GPR179*, CSNB1, missense mutations, G-protein-coupled receptor, trafficking defect, pathogenicity

Congenital stationary night blindness (CSNB) is a clinically and genetically heterogeneous group of retinal disorders characterized by nonprogressive impairment of night vision and variable decrease in visual acuity. The Schubert-Bornschein class of CSNB is caused by defective signaling from photoreceptors to bipolar cells (BCs), and is characterized by a reduced or absent b-wave but a normal a-wave in the electroretinogram (ERG). Two types of Schubert-Bornschein CSNB can be distinguished by using the standard flash ERG: "complete" or type 1 CSNB (CSNB1, OMIM 310500) and "incomplete" or type 2 CSNB (CSNB2, OMIM 300071).¹ CSNB1 is characterized by a complete lack of rod pathway function. CSNB2 is characterized by abnormal rod pathway function in addition to impaired cone

pathway function. These distinct phenotypes reflect the location of the mutated proteins. CSNB2 is caused by mutations in genes expressed in photoreceptor terminals, while CSNB1 is caused by postsynaptic defects in depolarizing or ON-BCs.²⁻¹⁰

CSNB1 is caused by mutations in genes that are expressed in ON-BCs: *NYX*, which encodes nyctalopin, a leucine-rich proteoglycan of unknown function^{3,11,12}; *LRR3*, which also encodes a leucine-rich protein of unknown function¹³; *GRM6*, which encodes the metabotropic glutamate receptor 6 (mGLUR6)^{5,6}; and *TRPM1*, which encodes the transient receptor potential cation channel M1.^{8,10,14,15} Nyctalopin, *LRR3*, mGLUR6, and *TRPM1* are all localized on the dendrites of ON-BCs^{2,8,13,15-18} and are required for signal transmission

TABLE. Clinical Characteristics of CSNB1 Patients With *GPR179* Mutations

Patient	Sex	Age, y	Visual Acuity, logMAR		Nystagmus	Refractive Error, Spherical Equivalent		Dark-Adapted Threshold Elevation, log Units
			RE	LE		OD	OS	
HS	F	18	0.2	0.5	Present	−9.0	8.5	3
PS	M	15	0.15	0.15	Present	−8.0	7.0	3

RE, right eye; LE, left eye.

from photoreceptors to ON-BCs. This suggests a close interaction of these proteins within a single signaling cascade.

The rod pathway strongly depends on ON-BCs because at low scotopic intensities, the dark-adapted response is dominated by the primary rod pathway (rod → rod ON-BC → All amacrine cell pathway), whereas at higher stimulus levels the response is dominated by the secondary rod pathway (rod → cone (via gap junctions between rod and cone pedicles) → cone ON- and OFF-BC).^{19,20} Finally, there may be a tertiary pathway for rod signaling (rod → cone OFF-BCs).^{6,21,22} The 15-Hz flicker ERG paradigm has been used to obtain insight into dysfunction in these various rod pathways,^{6,8,21,22} as the signals generated by each rod pathway have different sensitivity and phase relations. In normal subjects, these pathways interact algebraically in a stereotypic fashion.²³ Interestingly, in contrast to the standard flash ERG, a 15-Hz flicker ERG paradigm is able to distinguish CSNB1 patients with *GRM6* mutations from CSNB1 patients with mutations in either *NYX* or *TRPM1*.^{6,8} Given current thinking about the role that these proteins play in ON-BC signaling, the 15-Hz flicker ERG appears to discriminate between the mGluR6 receptor complex and the TRPM1 channel complex (including nyctalopin). The origin of this difference is poorly understood.^{8,24}

Recently, we and others identified GPR179, an orphan G-protein receptor, as an important component of the ON-BC signaling cascade.^{9,25} The function of GPR179 has not been resolved but it seems to interact with mGluR6, suggesting a regulatory function in the cascade.²⁶ This article addresses 3 questions: (1) What is the ultrastructural localization of GPR179 in the human retina, (2) How is the human 15-Hz flicker ERG affected by mutations in *GPR179*, and (3) How closely do 15-Hz flicker ERG abnormalities in mouse models of CSNB1 resemble those reported in human patients? We found that GPR179 is localized at the tips of the ON-BCs, with localization similar to that for mGluR6 and TRPM1. Furthermore, we found that the 15-Hz flicker ERG abnormalities of patients with *GPR179* mutations resemble those in patients with mutations in either *NYX* or *TRPM1*, suggesting that loss of function of either GPR179, TRPM1, or nyctalopin results in a similar disturbance of the ON-BC cascade. Finally, we noted that the 15-Hz flicker ERG abnormalities are similar in *Gpr179^{nob5/nob5}* and *Grm6^{nob3/nob3}* mice, unlike the situation in humans, suggesting that the balance between the various rod pathways in humans and mice differ.

MATERIALS AND METHODS

Participants

CSNB1 was diagnosed by means of a complete ophthalmologic and electrophysiological examination, including funduscopy and measurements of dark-adapted thresholds. We analyzed samples from the 2 probands by direct sequencing. None had mutations in *GRM6*, *TRPM1*, or *NYX*. Once mutations in *GPR179* were identified, samples from first-

degree relatives were obtained and screened. All participants and/or their legal representatives gave permission to draw blood for mutation analyses. Patient studies were conducted in accordance with the principles outlined in the Declaration of Helsinki.

All procedures used in animal experiments were approved by the Institutional Animal Care & Use Committees of the Cleveland Clinic and were in agreement with the ARVO Statement for the Use of Animals in Ophthalmic and Vision Research. *Gpr179^{nob5}* and *Grm6^{nob3}* mice were obtained from local breeding colonies.^{9,27} Control mice were C57B2/6, obtained from The Jackson Laboratory (Bar Harbor, ME) or heterozygous littermates.

Human Retinal Material

This study was performed in agreement with the Declaration of Helsinki on the use of human material for research. Postmortem human donor eyes were obtained from the Euro Tissue Bank. In accordance with Dutch law, the Euro Tissue Bank ensured none of the donors objected to the use of their eyes for scientific purposes.

Light and Electron Microscopy

The sclera and corpus vitreous were peeled away and the retinas were fixed in 4% paraformaldehyde buffered in 0.1 M phosphate buffer (PB) at pH 7.4 for 30 to 60 minutes. Retinas were cryoprotected in 12.5% sucrose in 0.1 M PB for 30 minutes, followed by 1 hour in 25% sucrose in 0.1 M PB, and finally frozen in Tissue Tek (Sakura Finetek Europe B.V., Leiden, The Netherlands).

For light microscopy, 10- μ m-thick sections were cut and stored at -20°C . The sections were preincubated in 2% normal goat serum (NGS) for 30 minutes and incubated for 24 to 48 hours in 0.1 M phosphate-buffered saline (PBS) containing 5% NGS and 0.05% Triton X-100 with the following primary antibodies: GPR179 (1:200; Sigma, Zwijndrecht, The Netherlands), calbindin (1:500; Swant, Bellinzona, Switzerland), G α (1:1000; Chemicon, Amsterdam, The Netherlands), and PKC α (1:200; Sigma). The sequence against which the GPR179 antibody was raised is as follows: LNMLLQAN-DIRESSVEEDVEWYQALVRSVAEGDPRVYRALLTFNPPP-GASHLQLALQATRTGEETILQDLSGNWNVQEEENPPGDLDT-PALKKRVLNLDLGLSPKWPQADGYVGDQVRLSPPFLEC-QEGRLRPGWLITLSATF. The sections were washed 3 times for 5 minutes each in PBS, and secondary antibodies (1:500, goat anti-rabbit Cy3; or 1:500, goat anti-mouse Alexa 488) were applied for 35 minutes at 37°C . Sections were examined with a Zeiss CSLM meta confocal microscope (Jena, Germany).

For electron microscopy (EM), 40- μ m-thick sections were incubated with antibodies to GPR179 (1:200) in PB for 48 hours. After rinsing, the sections were incubated in anti-rabbit conjugated peroxidase anti-peroxidase antibody for 2 hours following a 4 minute development in a 2,2'-diaminobenzidine solution containing 0.03 % H_2O_2 . Next, we followed the gold substitute silver peroxidase method.²⁸ Finally, the sections

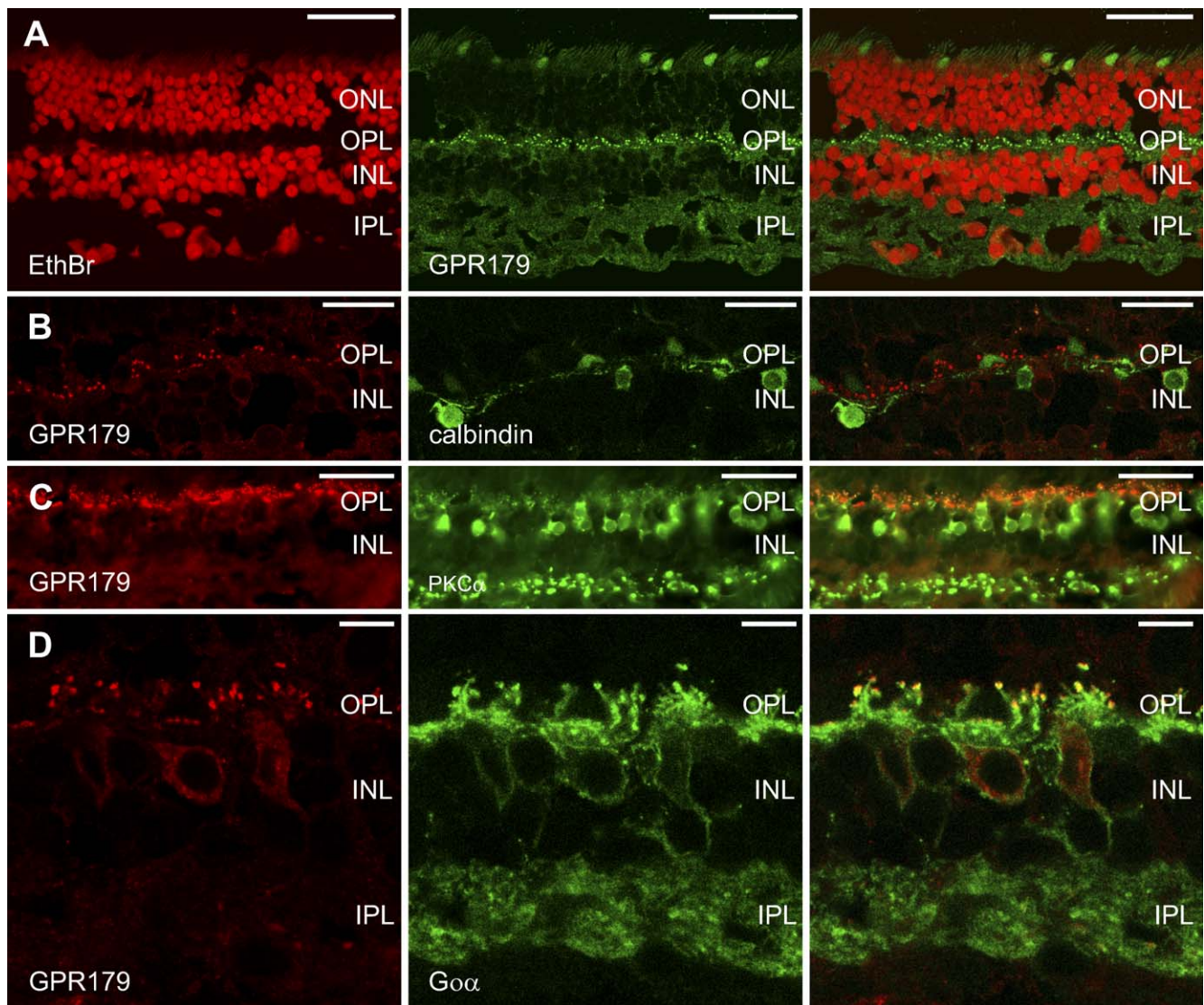


FIGURE 1. GPR179 colocalizes with markers for ON-BCs but not for HCs. *Left and middle columns* show the individual channels while the *right column* shows the combination of the 2 channels. (A) Immunohistochemical localization of GPR179 (green) in the human retina. Nuclei (red) were stained with ethidium bromide. Note the punctate labeling in the OPL and diffuse, nonspecific labeling in the IPL. (B) Retinal section labeled with antibodies against GPR179 (red) and calbindin (green). Calbindin labels some HC types. No calbindin labeling could be detected in ON-BCs. Calbindin-IR does not overlap with GPR179-IR, suggesting that GPR179 is not expressed by HCs or OFF-BCs. (C) Retinal section labeled with antibodies to GPR179 (red) and PKC α (green). PKC α labels rod-BCs and colocalization is seen at the tips of the ON-BC dendrites. (D) Retinal section labeled with antibodies to GPR179 (red) and Go α (green). Go α labels ON-BCs and colocalization was found at the tips of the ON-BC dendrites. *Scale bars:* 50 μ m (A, C), 15 μ m (B), 5 μ m (D). ONL, outer nuclear layer; INL, inner nuclear layer.

were fixated in sodium cacodylate buffer (pH 7.4) containing 1% osmium tetroxide and 1.5% potassium ferricyanide, dehydrated and embedded in Epoxy resin. Uranylacetate and lead citrate were used to enhance contrast. Ultrathin sections were examined with a FEI Tecnai 12 electron microscope (FEI, Eindhoven, The Netherlands).

ERG Studies in Humans

Electroretinograms were recorded by using DTL-electrodes and were in accordance with recommendations of the International Society for Clinical Electrophysiology of Vision for extended protocols. Stimuli were produced by a Ganzfeld stimulator (Colordome system; Diagnosys LLC, Impington, Cambridge, UK). In addition, we recorded 15-Hz flicker ERGs to examine the function of the various rod pathways.^{6,21,22}

Flash luminance ranged from -2.3 to 1.7 log scot td \cdot s, assuming a pupil diameter of 8 mm, in steps of approximately 0.4 log scot td \cdot s. The clinical characteristics of the patients with GPR179 mutation are shown in the Table. Funduscopy showed myopic changes and optical coherence tomography analysis of the retina was normal in both patients.

ERG Studies in Mice

After overnight dark adaptation, mice were anesthetized with ketamine (80 mg/kg) and xylazine (16 mg/kg) and their pupils were dilated with 1% tropicamide and 2.5% phenylephrine HCl eyedrops. The cornea was anesthetized with 1% proparacaine HCl. Electroretinograms were recorded by using a stainless steel wire contacting the corneal surface. The reference needle electrode was placed in the cheek, and the ground needle

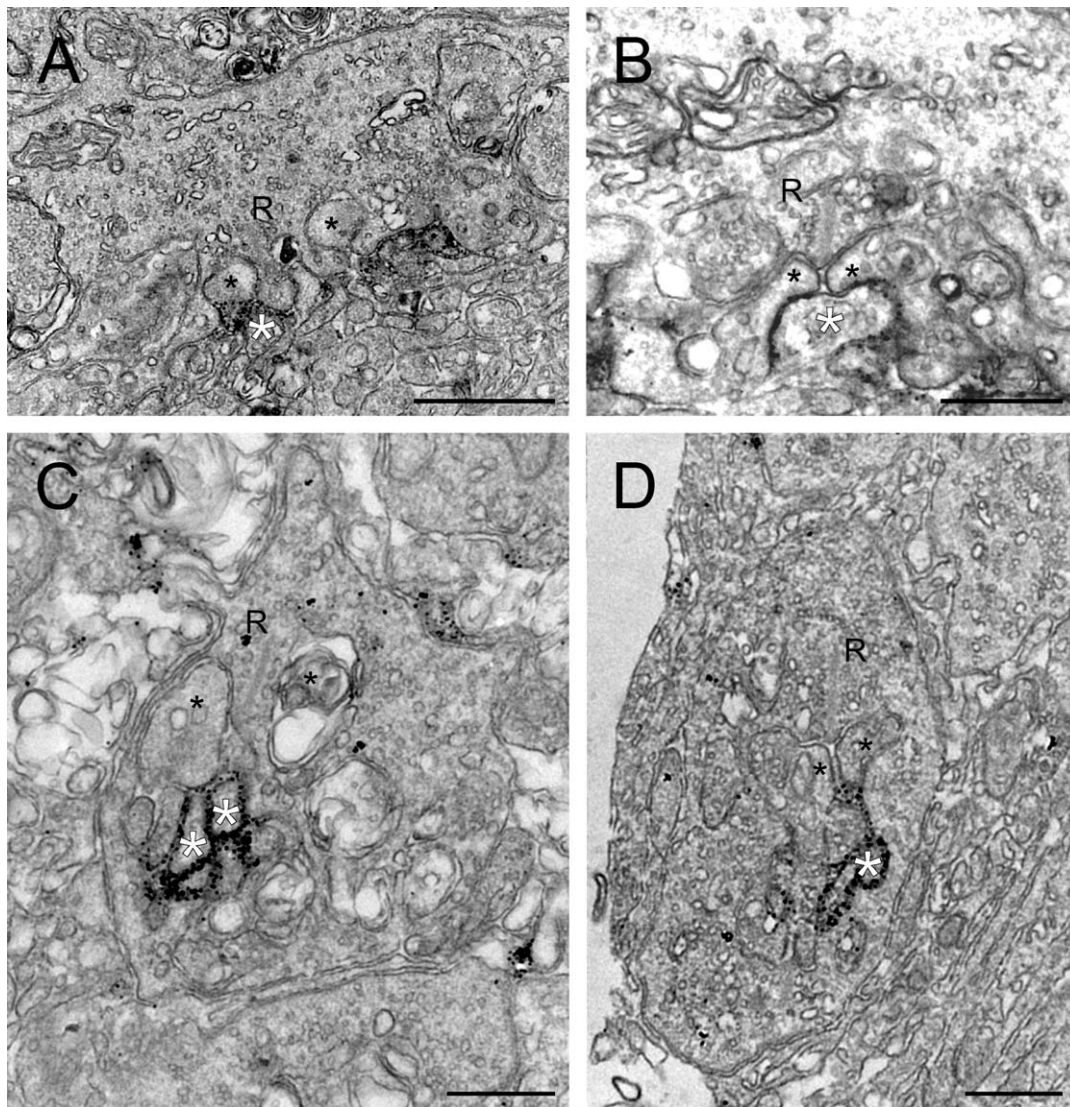


FIGURE 2. Ultrastructural localization of GPR179 in the human retina. (A, B) Human cone pedicles showing labeling for GPR179 on ON-BC dendrites. The *black spots* indicate GPR179-IR and are found around the invaginating ON-BC dendrites (*white asterisks*). Labeling was not observed in the HC dendrites (*black asterisks*). (C, D) Human rod terminals showing labeling for GPR179 on ON-BC dendrites. GPR179-IR is found in rod terminals, around the invaginating ON-BC dendrites (*white asterisks*) and not the lateral HC dendritic elements (*black asterisks*). Scale bars: 1 μ m (A), 500 nm (B-D). R, synaptic ribbon.

electrode was placed in the tail. Responses were amplified, filtered (0.03–1000 Hz) and stored by using an LKC (Gaithersburg, MD) UTAS E-3000 signal averaging system. Stimuli were presented at 15 Hz. Amplitude and phase were derived by a Fast Fourier Transformation algorithm applied to the averaged signal.

RESULTS

Localization of GPR179

GPR179 has been localized to the dendrites of ON-BCs in mice.⁹ However, the ultrastructural localization has not been determined. We first examined the expression pattern of GPR179 in the human retina at the light microscopic level. Figure 1A shows immunoreactivity (IR) of GPR179 (green) in the human retina. The red label is a nuclear stain (ethidium bromide). GPR179-IR revealed a specific punctate staining pattern in the outer plexiform layer (OPL) (Fig. 1A, green)

characteristic for the dendritic tips of ON-BCs. Some faint, diffuse labeling was also visible in the inner plexiform layer (IPL). Since this labeling was not punctate, we conclude that it is nonspecific background labeling. We next performed a series of double-labeling experiments to determine whether the GPR179-IR in the OPL was associated with the dendritic tips of ON-BCs. Figures 1B through 1D show retinal sections double labeled for GPR179 (red) and either calbindin (Fig. 1B) or PKC α (Fig. 1C) or Go α (Fig. 1D). In primates calbindin-IR is present in some horizontal cell (HC) and OFF-BC types.^{29,30} Figure 1B illustrates that the GPR179-IR (red) and calbindin-IR (green) do not colocalize, showing that GPR179 is not expressed by HC dendrites. On the other hand PKC α (rod BCs)³¹ and Go α (all ON-BCs)³² colocalize with GPR179 as puncta in the OPL (Figs. 1C, 1D), suggesting expression of GPR179 at the tips of the dendrites of rod and cone ON-BCs. This expression pattern of GPR179 is similar to that seen in mouse retina.⁹

To validate this conclusion, we used pre-embedding immuno-electron microscopy (Fig. 2). At the EM level, the synaptic complexes of rod and cone photoreceptors can be identified by their characteristic triadic synaptic structure with ON-BCs and HCs.^{33,34} The elements ending lateral of the synaptic ribbon are dendrites of HCs, whereas the elements ending opposite to the synaptic ribbon are dendrites of ON-BCs.

The cone synaptic complex involves multiple ribbon synapses. Figure 2A shows a cone terminal with GPR179-IR present in ON-BC-dendrites (white asterisks). Horizontal cell dendrites are devoid of labeling (black asterisks). Figure 2B shows a higher magnification of a cone synaptic terminal where a ribbon synapse (R) can be identified. GPR179-IR was present on the central elements opposed to the ribbon (white asterisks), whereas it was never found on the lateral elements of HCs (black asterisks). The finding that GPR179-IR was only found on invaginating processes and not at flat contacts at the base of the cone pedicle indicates that GPR179 is not expressed by OFF-BCs.³⁵

Figures 2C and 2D show rod synaptic terminals characterized by only 1 synaptic ribbon. GPR179-IR was present on the central element of the triad (white asterisks), whereas the lateral elements (black asterisks) never showed any labeling. This suggests that GPR179 was localized to the dendrites of ON-BCs invaginating the rod spherule. These immunocytochemical and ultrastructural findings showed that GPR179 is located on the tips of the ON-BC dendrites that invaginate rods and cones similar to the location of TRPM1¹⁸ and mGLUR6.¹⁶

Human ERG

What is the functional impact of the loss of GPR179? The 15-Hz flicker ERG has been shown to discriminate between patients with mutations in *GRM6* and those with mutations in *TRPM1* and *NYX*.^{6,8} In view of recent evidence indicating that mGluR6 and GPR179 may interact,²⁶ we hypothesized that *GPR179* mutations may lead to a 15 Hz-flicker ERG phenotype that resembles that seen in *GRM6* patients.

Figure 3A shows a series of dark-adapted ERG responses obtained from a normal control subject and 2 patients with homozygous p.Tyr220Cys mutations in *GPR179*. In response to low-luminance stimuli, ERGs of both patients were indistinguishable from noise. At higher stimulus luminance, both patients generated an ERG with normal a-wave amplitude but no b-wave (Fig. 3A). These ERG abnormalities are characteristic of defective ON-BC pathway signaling.³⁶ In both patients, the light-adapted 30-Hz flicker ERG (Fig. 3B, top traces) was similar in amplitude and implicit time as seen in normal subjects. The amplitudes of the single-flash photopic responses (Fig. 3B, bottom traces) also were within the normal range. However, their shape seemed to have a square wave appearance indicating that cone ON-BCs are also involved, which is typical for CSNB1.³⁷

Figure 3C shows the 15-Hz ERG responses from a normal subject and CSNB1 patients HS and PS. In both patients, responses were absent at the lowest luminance levels, and a clear response was only obtained at stimulus luminance values of $-1.1 \log \text{scot td} \cdot \text{s}$ and higher. The amplitude minimum of control subjects occurred near $-1.1 \log \text{scot td} \cdot \text{s}$ (Fig. 3C, arrow). Above this stimulus level, the 15-Hz flicker ERG responses of patients increased in amplitude and, at the highest stimulus luminance, fell within the range of control subjects (Fig. 3D). In both patients, the phase of the responses remained stable over an $\sim 3 \log$ unit range of luminance, whereas in controls the phase progressively advanced with increasing luminance. In the patients, the overall waveform of the 15-Hz flicker ERG presented with a more "square wave"

appearance of the a-wave, particularly at the higher stimulus luminance (Fig. 3C). Overall, these 15-Hz flicker ERG data resemble more closely those of *NYX* and *TRPM1* patients than those of *GRM6* patients.⁸

Mouse ERG

Are the 15-Hz flicker ERG responses in CSNB1 patients comparable to those found in mouse models of CSNB1? Figure 4 shows the 15-Hz flicker ERGs of control and *Gpr179^{nob5}* mice. The control mouse 15-Hz flicker ERG roughly resembled that of humans. The response amplitude increased with increasing luminance until approximately $-1 \log \text{cd s/m}^2$ where it reached a maximum and then decreased with increasing luminance. A minimum was reached at $\sim 0 \log \text{cd s/m}^2$, after which it increased again (Fig. 4A).³⁸ There are, however, important differences between the human and the control mouse 15-Hz flicker ERGs. For example, the range over which the response increases at low light levels is much broader in the mouse than in human. In *Gpr179^{nob5}* mice the response amplitudes only became significant above approximately $-0.5 \log \text{cd s/m}^2$ and were always reduced in comparison to those of control mice (Figs. 4A, 4B). This is in contrast to humans where at high luminance levels the 15-Hz flicker ERG amplitudes in CSNB1 patients fell within the normal range (Fig. 3D). As in humans, the control mouse response function (Fig. 4B left, black line) was characterized by 2 peaks. The initial peak was absent in *Gpr179^{nob5}* mice and the second peak had an onset approximately 0.5 log unit below the control minimum. Figure 4B (right, blue curves) shows the phase characteristics. The control mouse phase characteristics resemble those of humans: a gradual phase shift with increasing luminance. The phase of the *GPR179^{nob5}* ERGs shifted with increasing luminance, but never matched that of control. This behavior differs from that of the patients, where the response phase remained stable across an $\sim 3 \log$ unit stimulus range (Fig. 3D). To determine if the 15-Hz flicker ERG could distinguish between *GRM6* and *GPR179* mouse mutants, we tested *Grm6^{nob3}* mice. Both amplitude and phase measures matched closely those of *Gpr179^{nob5}* mutants (Fig. 4B, red curves).

DISCUSSION

The present study demonstrated the expression pattern and ultrastructural localization of GPR179 in human retina. GPR179 is localized in puncta in the OPL, specifically on the dendritic tips of the ON-BCs. This location matches that of all other proteins implicated in CSNB1 (nyctalopin, mGLUR6, TRPM1, and LRIT3)^{2,8,13,15-18} and the expression pattern of GPR179 in mice.⁹ Our ultrastructural data showed that in human retina GPR179 is located postsynaptically, on the dendrite tips of ON-BCs near synaptic ribbons of both cone and rod synaptic terminals. This localization is consistent with the known localization of several other proteins involved in the ON-BC signaling cascade. In primate, mouse, and now human retina mGLUR6,^{39,40} nyctalopin,² TRPM1,^{8,14,17,18} *Goα*³² and, as shown here, GPR179,⁹ are all found on the central element of the triads close to the synaptic ribbons in both rods and cones. These data suggest that all these proteins are part of a single signaling complex. Recently, it has been shown that mutations in LRIT3¹³ cause CSNB1, suggesting that this protein is also involved in the ON-BC signaling cascade. Ultrastructural localization of LRIT3 awaits further study. The role of GPR179 in the ON-BC signal cascade is an area of active interest and its function and the interacting proteins have not been fully

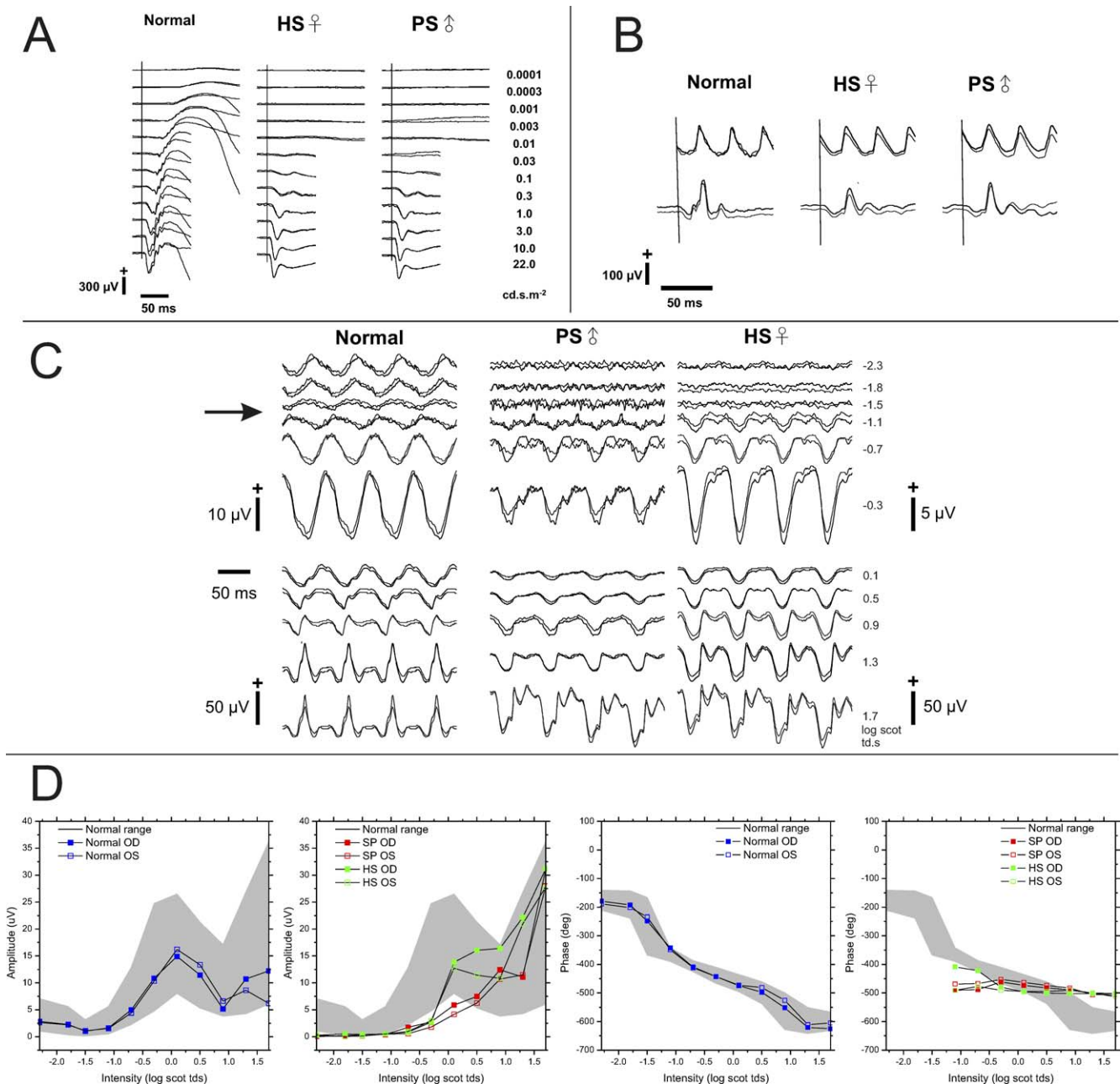


FIGURE 3. Standard and 15-Hz flicker ERG obtained from a normal subject and 2 patients with GPR179 mutations. **(A)** Dark-adapted flash ERGs. Both patients lack the dark-adapted b-wave, but retain a normal a-wave. **(B)** Light-adapted ERGs to 3 cd s m^{-2} ; strobe flashes superimposed on a steady 30 cd s m^{-2} adapting field. The amplitudes of the 30-Hz flicker ERG (top trace) and the single-flash photopic ERGs fall within the normal range. The a-wave has a “square wave” appearance. **(C)** 15-Hz scotopic ERGs. Responses at low flash luminance levels present in control subjects are absent in patients. In patients, the responses first appear at $-1.1 \text{ log scot td} \cdot \text{s}$, near the initial amplitude minimum of control subjects, and then grow with increasing stimulus luminance. **(D)** 15-Hz ERG amplitude and phase data. The grey area indicates the mean $\pm 2 \text{ SD}$ for 20 normal control subjects.^{21,22} Response amplitudes for patients remain below the normal range until high luminance stimuli are used. When measurable responses were recorded from patients they retained constant phase through an $\sim 3 \text{ log unit}$ luminance range.

resolved, although it is required for normal expression of RGS7 and RGS11.⁴¹

15-Hz Flicker ERG

In normal subjects, the 15-Hz flicker ERG amplitude decreases with increasing stimulus luminance, reaches a null at approximately $-1.5 \text{ log scot td} \cdot \text{s}$ before increasing again at higher luminance.^{21,22} This behavior of the 15-Hz flicker ERG is due to destructive interference, caused by out-of-phase

signals from the primary and secondary rod pathways.²⁰ At low light intensities the 15-Hz flicker ERG is dominated by the primary rod pathway, whereas at high intensities it is dominated by the cone pathway. In the range of $-1.5 \text{ log scot td} \cdot \text{s}$ the primary and the secondary rod pathways are about equally sensitive but out of phase, while the cone pathway is not yet functioning. The result is that at this luminance level the 2 signals cancel each other and the amplitude is decreased. In CSNB1 patients the primary rod pathway is absent so one would expect an altered 15-Hz flicker ERG. In CSNB1 patients

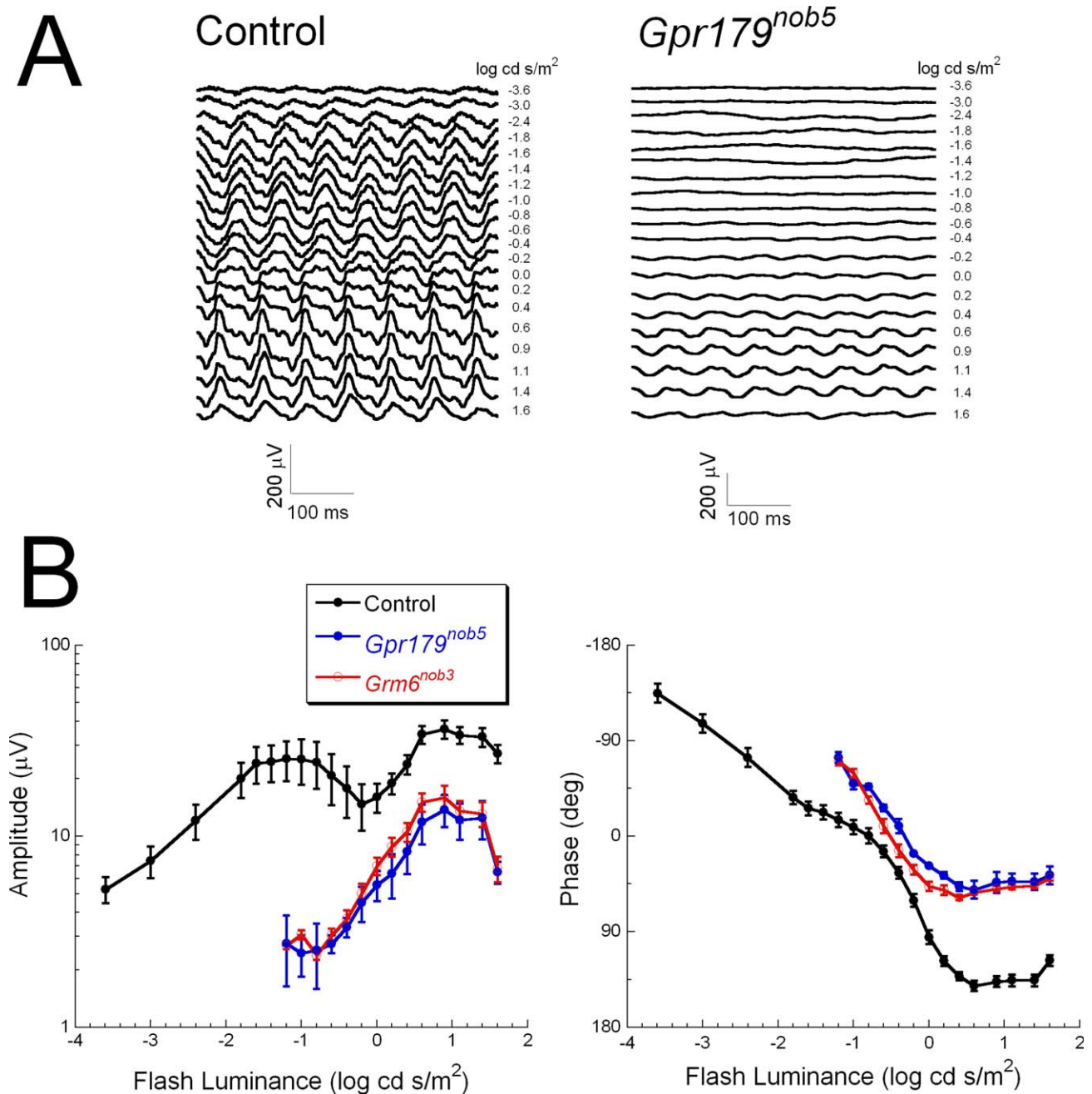


FIGURE 4. Mouse 15-Hz flicker ERGs (A) Representative 15-Hz flicker ERGs obtained from a control mouse (left) and a $Gpr179^{nob5}$ mouse (right). Stimulus luminance is indicated to the right of each waveform. (B) Average (\pm SEM) amplitude (left) and phase (right) plots obtained from 7 control (black), 4 $Gpr179^{nob5}$ (blue), and 4 $Grm6^{nob3}$ (red) mice.

with mutations in *TRPM1* or *NYX* responses were absent at low luminance levels, but at higher luminance levels the responses are similar in amplitude to those of normal subjects.⁸ The phase of the 15-Hz flicker ERG responses in these CSNB1 patients is shifted relative to the phase of the responses of normal subjects. From these data the authors concluded that in CSNB1 patients the primary rod pathway function is completely absent and that the activity of the secondary rod pathway is mildly reduced.⁶ Surprisingly, patients with mutations in *GRM6* had responses at all luminance levels, but the phase behavior strongly differed from that of normal subjects. The underlying mechanism for this difference in phase behavior has not yet been established; however, the 15-

Hz flicker ERG does discriminate patients with mutations in components of the receptor complex (mGLUR6) and the channel complex (nyctalopin, TRPM1).⁸

Our human studies showed that the functional consequences of mutations in *GPR179* result in a 15-Hz flicker ERG phenotype similar to that of CSNB1 patients with mutations in *TRPM1* or *NYX*. Patients with mutations in *GPR179*, *TRPM1*, or *NYX* lack all responses in the scotopic range,⁸ whereas those with mutations in *GRM6* retain a low luminance signal.^{6,8} *TRPM1* and *NYX* mutations both result in a nonfunctional or absent channel.⁴² The fact that 15-Hz flicker ERG abnormalities in patients with *GPR179* mutations are similar to those with *TRPM1* or *NYX* mutations suggests that

the loss of GPR179 leads to the loss or closure of TRPM1 channel. Because activation of mGluR6 closes the TRPM1 channel, we postulate that in the absence of mGluR6, TRPM1 channels remain constitutively open. To date, however, the number of fully characterized human patients with GPR179 mutations is quite small; it will be important to analyze additional patients to determine if this generalization holds true.

A surprising result of the present study is that in contrast to the human studies, mice with mutations in either *Gpr179* or *Grm6* had very similar 15-Hz flicker ERGs even though the current evidence indicates the ON-BC signaling cascade in mice and humans is highly conserved.^{6,8,9,12} The standard flash ERGs were also comparable. Given that the 15-Hz responses of patients with *GRM6* mutations are thought to reflect activity of a spared tertiary rod pathway, the present results suggest that such a tertiary rod pathway is less pronounced or even completely absent in mice. Alternatively, it may not be possible to monitor the tertiary pathway by recording at the mouse corneal surface. Prior ERG studies also indicate that the relative contributions of retinal cell types to the corneal ERG differ between mice and humans. For example, while both human and mouse retinas contain OFF-BCs,⁴³ the relative contribution of OFF-BCs in the primate ERG is much larger⁴⁴⁻⁴⁶ than in the rodent ERG.^{47,48}

Nusinowitz and coworkers³⁸ have also shown that the minimum in the 15-Hz flicker ERG is less pronounced in mice than in humans and that the frequency range where destructive interference occurs in mice (10–20 Hz) is larger than in humans (14–16 Hz). This range difference is not the origin of the less-pronounced minimum since it is smaller for all tested frequencies.³⁸ Therefore, both the published and our new data suggest that the relative contribution of the primary and secondary rod pathways in control mice might differ considerably from that in humans.

Acknowledgments

The authors thank the Euro Tissue Bank for supplying the human retinas.

Supported by a grant by ODAS (ERG studies in the CSNB patients), National Institutes of Health R01 EY12354 (RGG) and R21 EY21852 (NSP, RGG), the Foundation Fighting Blindness, the Department of Veterans Affairs, and unrestricted grants from Research to Prevent Blindness to the University of Louisville and the Cleveland Clinic Lerner College of Medicine of Case Western Reserve University.

Disclosure: **J. Klooster**, None; **M.M. van Genderen**, None; **M. Yu**, None; **R.J. Florijn**, None; **F.C.C. Riemslag**, None; **A.A.B. Bergen**, None; **R.G. Gregg**, None; **N.S. Peachey**, None; **M. Kamermans**, None

References

- Miyake Y, Yagasaki K, Horiguchi M, Kawase Y, Kanda T. Congenital stationary night blindness with negative electroretinogram: a new classification. *Arch Ophthalmol*. 1986;104:1013–1020.
- Gregg RG, Kamermans M, Klooster J, et al. Nyctalopin expression in retinal bipolar cells restores visual function in a mouse model of complete X-linked congenital stationary night blindness. *J Neurophysiol*. 2007;98:3023–3033.
- Bech-Hansen NT, Naylor MJ, Maybaum TA, et al. Mutations in NYX, encoding the leucine-rich proteoglycan nyctalopin, cause X-linked complete congenital stationary night blindness. *Nat Genet*. 2000;26:319–323.
- Pusch CM, Zeitz C, Brandau O, et al. The complete form of X-linked congenital stationary night blindness is caused by mutations in a gene encoding a leucine-rich repeat protein. *Nat Genet*. 2000;26:324–327.
- Dryja TP, McGee TL, Berson EL, et al. Night blindness and abnormal cone electroretinogram ON responses in patients with mutations in the GRM6 gene encoding mGluR6. *Proc Natl Acad Sci U S A*. 2005;102:4884–4889.
- Zeitz C, van Genderen MM, Neidhardt J, et al. Mutations in GRM6 cause autosomal recessive congenital stationary night blindness with a distinctive scotopic 15-Hz flicker electroretinogram. *Invest Ophthalmol Vis Sci*. 2005;46:4328–4335.
- Li Z, Sergouniotis PI, Michaelides M, et al. Recessive mutations of the gene TRPM1 abrogate ON bipolar cell function and cause complete congenital stationary night blindness in humans. *Am J Hum Genet*. 2009;85:711–719.
- Van Genderen MM, Bijveld MMC, Claassen Y, et al. Mutations in TRPM1 are a common cause of complete congenital stationary night blindness. *Am J Hum Genet*. 2009;85:730–736.
- Peachey NS, Ray TA, Florijn R, et al. GPR179 is required for depolarizing bipolar cell function and is mutated in autosomal-recessive complete congenital stationary night blindness. *Am J Hum Genet*. 2012;90:331–339.
- Audo I, Kohl S, Leroy BP, et al. TRPM1 is mutated in patients with autosomal-recessive complete congenital stationary night blindness. *Am J Hum Genet*. 2009;85:720–729.
- Scholl HP, Langrova H, Pusch CM, Wissinger B, Zrenner E, Apfelstedt-Sylla E. Slow and fast rod ERG pathways in patients with X-linked complete stationary night blindness carrying mutations in the NYX gene. *Invest Ophthalmol Vis Sci*. 2001;42:2728–2736.
- Zeitz C, Minotti R, Feil S, et al. Novel mutations in CACNA1F and NYX in Dutch families with X-linked congenital stationary night blindness. *Mol Vis*. 2005;11:179–183.
- Zeitz C, Jacobson SG, Hamel CP, et al. Whole-exome sequencing identifies LRIT3 mutations as a cause of autosomal-recessive complete congenital stationary night blindness. *Am J Hum Genet*. 2013;92:67–75.
- Morgans CW, Zhang J, Jeffrey BG, et al. TRPM1 is required for the depolarizing light response in retinal ON-bipolar cells. *Proc Natl Acad Sci U S A*. 2009;106:19174–19178.
- Shen Y, Heimel JA, Kamermans M, Peachey NS, Gregg RG, Nawy S. A transient receptor potential-like channel mediates synaptic transmission in rod bipolar cells. *J Neurosci*. 2009;29:6088–6093.
- Vardi N, Morigiwa K. ON cone bipolar cells in rat express the metabotropic receptor mGluR6. *Vis Neurosci*. 1997;14:789–794.
- Bellone RR, Brooks SA, Sandmeyer L, et al. Differential gene expression of TRPM1, the potential cause of congenital stationary night blindness and coat spotting patterns (LP) in the Appaloosa horse (*Equus caballus*). *Genetics*. 2008;179:1861–1870.
- Klooster J, Blokker J, ten Brink JB, et al. Ultrastructural localization and expression of TRPM1 in the human retina. *Invest Ophthalmol Vis Sci*. 2011;52:8356–8362.
- Sharpe LT, Stockman A, MacLeod DI. Rod flicker perception: scotopic duality, phase lags and destructive interference. *Vision Res*. 1989;29:1539–1559.
- Stockman A, Sharpe LT, Ruther K, Nordby K. Two signals in the human rod visual system: a model based on electrophysiological data. *Vis Neurosci*. 1995;12:951–970.
- Bijveld MM, Riemslag FC, Kappers AM, Hoeben FP, van Genderen MM. An extended 15 Hz ERG protocol (2): data of normal subjects and patients with achromatopsia, CSNB1, and CSNB2. *Doc Ophthalmol*. 2011;123:161–172.
- Bijveld MM, Kappers AM, Riemslag FC, Hoeben FP, Vrijling AC, van Genderen MM. An extended 15 Hz ERG protocol (1): the

- contributions of primary and secondary rod pathways and the cone pathway. *Doc Ophthalmol*. 2011;123:149-159.
23. Sharpe LT, Stockman A. Rod pathways: the importance of seeing nothing. *Trends Neurosci*. 1999;22:497-504.
 24. Xu Y, Dhingra A, Fina ME, Koike C, Furukawa T, Vardi N. mGluR6 deletion renders the TRPM1 channel in retina inactive. *J Neurophysiol*. 2012;107:948-957.
 25. Audo I, Bujakowska K, Orhan E, et al. Whole-exome sequencing identifies mutations in GPR179 leading to autosomal-recessive complete congenital stationary night blindness. *Am J Hum Genet*. 2012;90:321-330.
 26. Orlandi C, Cao Y, Martemyanov K. Orphan receptor GPR179 forms macromolecular complexes with components of metabotropic signaling cascade in retina ON-bipolar neurons [published online ahead of print October 10, 2013]. *Invest Ophthalmol Vis Sci*. doi:10.1167/iovs.13-12907.
 27. Maddox DM, Vessey KA, Yarbrough GL, et al. Allelic variance between GRM6 mutants, Grm6nob3 and Grm6nob4 results in differences in retinal ganglion cell visual responses. *J Physiol*. 2008;586:4409-4424.
 28. Van den Pol AN, Gorcs T. Synaptic relationships between neurons containing vasopressin, gastrin-releasing peptide, vasoactive intestinal polypeptide, and glutamate decarboxylase immunoreactivity in the suprachiasmatic nucleus: dual ultrastructural immunocytochemistry with gold-substituted silver peroxidase. *J Comp Neurol*. 1986;252:507-521.
 29. Grunert U, Martin PR, Wassle H. Immunocytochemical analysis of bipolar cells in the macaque monkey retina. *J Comp Neurol*. 1994;348:607-627.
 30. Haverkamp S, Haeseleer F, Hendrickson A. A comparison of immunocytochemical markers to identify bipolar cell types in human and monkey retina. *Vis Neurosci*. 2003;20:589-600.
 31. Kolb H, Zhang L, Dekorver L. Differential staining of neurons in the human retina with antibodies to protein kinase C isozymes. *Vis Neurosci*. 1993;10:341-351.
 32. Vardi N. Alpha subunit of Go localizes in the dendritic tips of ON bipolar cells. *J Comp Neurol*. 1998;395:43-52.
 33. Missotten L. *The Ultrastructure of the Human Retina*. Brussels: Arscia Uitgaven N.V.; 1965.
 34. Dowling JE, Boycott BB. Organization of the primate retina: electron microscopy. *Proc R Soc Lond B Biol Sci*. 1966;166:80-111.
 35. Wassle H. Parallel processing in the mammalian retina. *Nat Rev Neurosci*. 2004;5:747-757.
 36. Sieving PA. Photopic ON- and OFF-pathway abnormalities in retinal dystrophies. *Trans Am Ophthalmol Soc*. 1993;91:701-773.
 37. Lachapelle P, Little JM, Polomeno RC. The photopic electroretinogram in congenital stationary night blindness with myopia. *Invest Ophthalmol Vis Sci*. 1983;24:442-450.
 38. Nusinowitz S, Ridder WH III, Ramirez J. Temporal response properties of the primary and secondary rod-signaling pathways in normal and Gnat2 mutant mice. *Exp Eye Res*. 2007;84:1104-1114.
 39. Nawy S. The metabotropic receptor mGluR6 may signal through G(o), but not phosphodiesterase, in retinal bipolar cells. *J Neurosci*. 1999;19:2938-2944.
 40. Morigiwa K, Vardi N. Differential expression of ionotropic glutamate receptor subunits in the outer retina. *J Comp Neurol*. 1999;405:173-184.
 41. Orlandi C, Posokhova E, Masuho I, et al. GPR158/179 regulate G protein signaling by controlling localization and activity of the RGS7 complexes. *J Cell Biol*. 2012;197:711-719.
 42. Pearring JN, Bojang P Jr, Shen Y, et al. A role for nyctalopin, a small leucine-rich repeat protein, in localizing the TRP melastatin 1 channel to retinal depolarizing bipolar cell dendrites. *J Neurosci*. 2011;31:10060-10066.
 43. Dowling JE. *The Retina: An Approachable Part of the Brain*. 1st ed. Cambridge: Belknap Press; 1987.
 44. Sieving PA, Murayama K, Naarendorp E. Push-pull model of the primate photopic electroretinogram: a role for hyperpolarizing neurons in shaping the b-wave. *Vis Neurosci*. 1994;11:519-532.
 45. Kondo M, Sieving PA. Primate photopic sine-wave flicker ERG: vector modeling analysis of component origins using glutamate analogs. *Invest Ophthalmol Vis Sci*. 2001;42:305-312.
 46. Khan NW, Kondo M, Hirianna KT, Jamison JA, Bush RA, Sieving PA. Primate retinal signaling pathways: suppressing ON-pathway activity in monkey with glutamate analogues mimics human CSNB1-NYX genetic night blindness. *J Neurophysiol*. 2005;93:481-492.
 47. Xu L, Ball SL, Alexander KR, Peachey NS. Pharmacological analysis of the rat cone electroretinogram. *Vis Neurosci*. 2003;20:297-306.
 48. Sharma S, Ball SL, Peachey NS. Pharmacological studies of the mouse cone electroretinogram. *Vis Neurosci*. 2005;22:631-636.